Tokyo Climate Center, Japan Meteorological Agency

TCC News

Spring 2025

Table of Contents: TCC News No. 80

JMA's Seasonal Numerical Ensemble Prediction for Boreal Summer 2025

This report outlines JMA's dynamical seasonal ensemble prediction for boreal summer 2025 (June – August, referred to as JJA), which was used as a basis for JMA's operational three-month outlook issued on 20 May 2025. The outlook is based on the seasonal ensemble prediction system of the coupled atmosphere-ocean general circulation model (CGCM).

Summary: Based on JMA's seasonal ensemble prediction system, it is likely (60%) that ENSO-neutral conditions will persist to boreal autumn. In association with above-normal sea surface temperatures (SSTs) from the tropical Indian Ocean to the western tropical Pacific, enhanced convection is expected from the eastern Indian Ocean to the Maritime Continent. In the lower troposphere, anti-cyclonic circulation anomalies straddling the equator are expected over the western Pacific in association with below-normal precipitation over the western equatorial Pacific.

1. Sea surface temperatures

Figure 1-1 shows predicted SSTs (contours) and related anomalies (shading) for JJA. Weak negative anomalies are expected around the central equatorial Pacific. The characteristics of warm water accumulation in the equatorial Pacific are unclear, and JMA's seasonal ensemble prediction system forecasts that NINO.3 SSTs will remain near normal until boreal autumn. In conclusion, it is likely (60%) that ENSO-neutral conditions will persist to boreal autumn. In the western tropical Pacific, positive anomalies are expected in boreal summer. In the tropical Indian Ocean, positive anomalies are expected over wide areas in boreal summer.

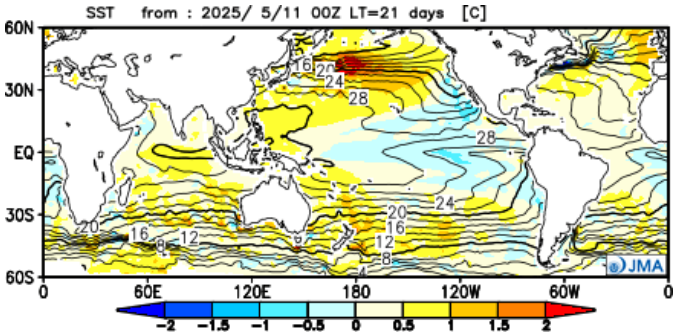

Figure 1-1 Predicted SSTs (contours) and SST anomalies (shading) for June–August 2025 (ensemble mean of 51 members)

2. Prediction for the tropics and sub-tropics

Figure 1-2 (a) shows predicted precipitation (contours) and related anomalies (shading) for JJA. Precipitation is expected to be above normal from the eastern Indian Ocean to the Maritime Continent and below normal over the western equatorial Pacific. The overall activity of the Asian summer monsoon is expected to be near normal, while the area of active convection over the western North Pacific is expected to shift northward of the normal, with above-normal precipitation along the 20°N latitude band.

Figure 1-2 (b) shows predicted velocity potential (contours) and related anomalies (shading) in the upper troposphere for JJA. Negative (i.e., large-scale divergence) anomalies are expected from Africa to the Maritime Continent, while positive (i.e., large-scale convergence) anomalies are expected from the central Pacific to South America.

Figure 1-2 (c) shows predicted stream functions (contours) and related anomalies (shading) in the upper troposphere for JJA. Anti-cyclonic circulation anomalies (i.e., positive in the Northern Hemisphere) straddling the equator are expected from the Atlantic to Africa in association with the above-mentioned divergence anomalies, implying a northwestward to northward extension of the Tibetan High. Cyclonic circulation anomalies straddling the equator are expected over the central Pacific in association with the above-mentioned convergence anomalies, implying a deepening and southwestward extension of the mid-Pacific trough over the subtropical North Pacific compared to the normal.

Figure 1-2 (d) shows predicted stream functions (contours) and related anomalies (shading) in the lower troposphere for JJA. Anti-cyclonic circulation anomalies straddling the equator are expected over the western Pacific in association with below-normal precipitation over the western equatorial Pacific. A tri-pole pattern of circulation anomalies is expected over the western North Pacific, with 1) anti-cyclonic circulation anomalies over the subtropical western North Pacific and to the south of the Kamchatka Peninsula and 2) relatively cyclonic circulation anomalies to the south of Japan. These anti-cyclonic circulation anomalies imply an enhanced southwestward and northward extension of the North Pacific subtropical high. The cyclonic circulation anomalies to the south of Japan correspond to above-normal precipitation along the 20°N latitude band over the western North Pacific.

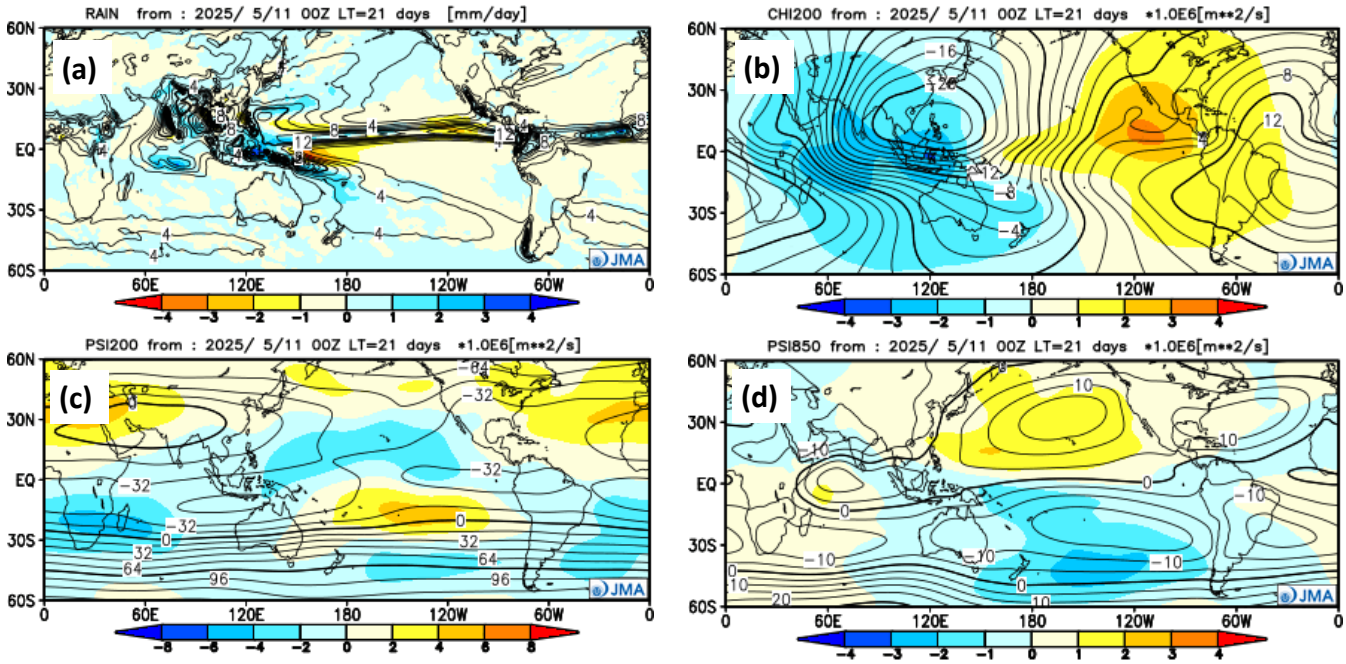

Figure 1-2 Predicted atmospheric fields over 60°N-60°S for June–August 2025 (ensemble mean of 51 members)

(a) Precipitation (contours) and anomaly (shading). The contour interval is 2 mm/day. (b) Velocity potential at 200-hPa (contours) and anomaly (shading). The contour interval is 2 × 10^6 m^2/s. (c) Stream function at 200-hPa (contours) and anomaly (shading). The contour interval is 16 × 10^6 m^2/s. (d) Stream function at 850-hPa (contours) and anomaly (shading). The contour interval is 5 × 10^6 m^2/s.

3. Prediction for the mid- and high- latitudes of the Northern Hemisphere

Figure 1-3 (a) shows predicted 500-hPa geopotential heights (contours) and related anomalies (shading) for JJA. Positive anomalies are expected over wide areas of the Northern Hemisphere, particularly to the west of Europe, to the north of Central Siberia and from the Sea of Okhotsk to eastern North America. Negative anomalies are expected over parts of Western Russia.

Figure 1-3 (b) shows predicted sea level pressure (contours) and related anomalies (shading) for JJA. Anomalies are expected to be positive over the subtropical North Pacific and negative over wide areas of Eurasia.

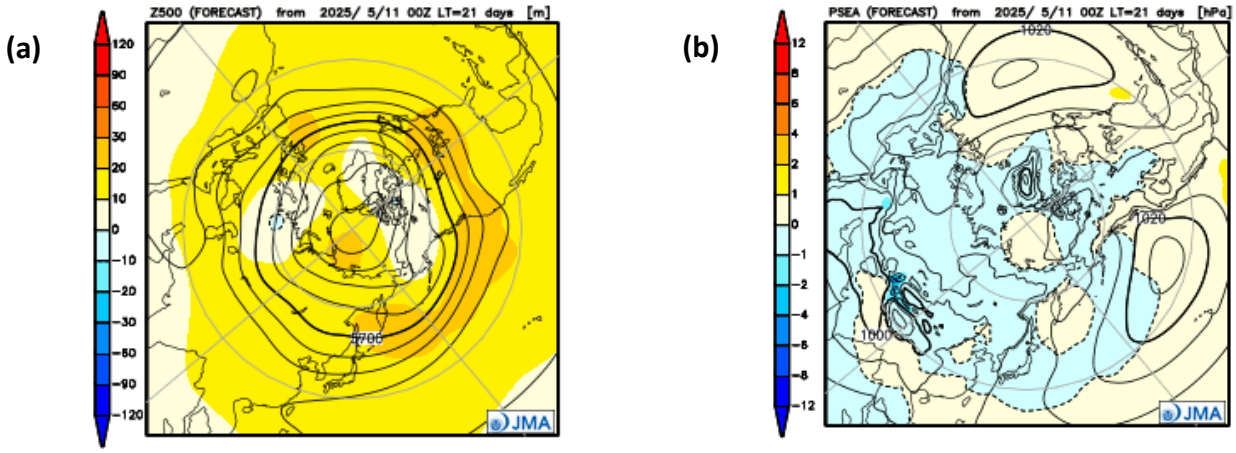

Figure 1-3 Predicted atmospheric fields over 20°N-90°N for June–August 2025 (ensemble mean of 51 members)
(a) Geopotential height at 500-hPa (contours) and anomaly (shading). The contour interval is 60 m. (b) Sea level pressure (contours) and anomaly (shading). The contour interval is 4 hPa.

Note: JMA operates a seasonal Ensemble Prediction System (EPS) using the Coupled atmosphere-ocean General Circulation Model (CGCM) to make seasonal predictions beyond a one-month time range. The EPS produces perturbed initial conditions by means of a combination of the initial perturbation method and the lagged average forecasting (LAF) method. Prediction is made using 51 members from the latest 17 initial dates (3 members are used every day). Details of the prediction system and verification maps based on 30-year hindcast experiments (1991–2020) are available at https://ds.data.jma.go.jp/wmc/products/model/.

(TAKEMURA Kazuto, Tokyo Climate Center)

<<Table of contents <Top of this article

Summary of the 2024/2025 Asian Winter Monsoon

This report summarizes the characteristics of the surface climate and atmospheric/oceanographic conditions related to the Asian winter monsoon for 2024/2025.

Note: Dataset of the Japanese Reanalysis for Three Quarters of a century (JRA-3Q) (Kosaka et al. 2024) and MGDSST (Kurihara et al. 2006) were used to analyze atmospheric circulation and sea surface temperature (SST). NOAA Climate Prediction Center (CPC) Blended Outgoing Longwave Radiation (OLR) data provided by the U.S. NOAA Physical Sciences Laboratory (PSL) from their web site at https://psl.noaa.gov/data/gridded/data.cpc_blended_olr-2.5deg.html was used to infer tropical convective activity. The base period for the normal is 1991 to 2020. The term "anomaly" as used in this report refers to deviation from the normal.

1. Surface climate conditions

In winter 2024/2025, three-month (DJF) mean temperatures were above normal over wide areas of Siberia, southern parts of South Asia and wide areas of the Maritime Continent, and below normal over parts of East Asia (Figure 2-1 (a)). Above-normal temperatures over Siberia were observed particularly in December and January (Figures 2-1 (b) and (c)), indicating weaker-than-normal accumulation of cold air masses over the area. Below-normal temperatures were particularly observed over western East Asia in December and southwestern Japan in February (Figures 2-1 (b) and (d)), indicating enhanced cold air outflow toward East Asia. Winter precipitation amounts were generally above normal over wide areas of Siberia and the Maritime Continent, and below normal over wide areas of East Asia (Figure 2-2).

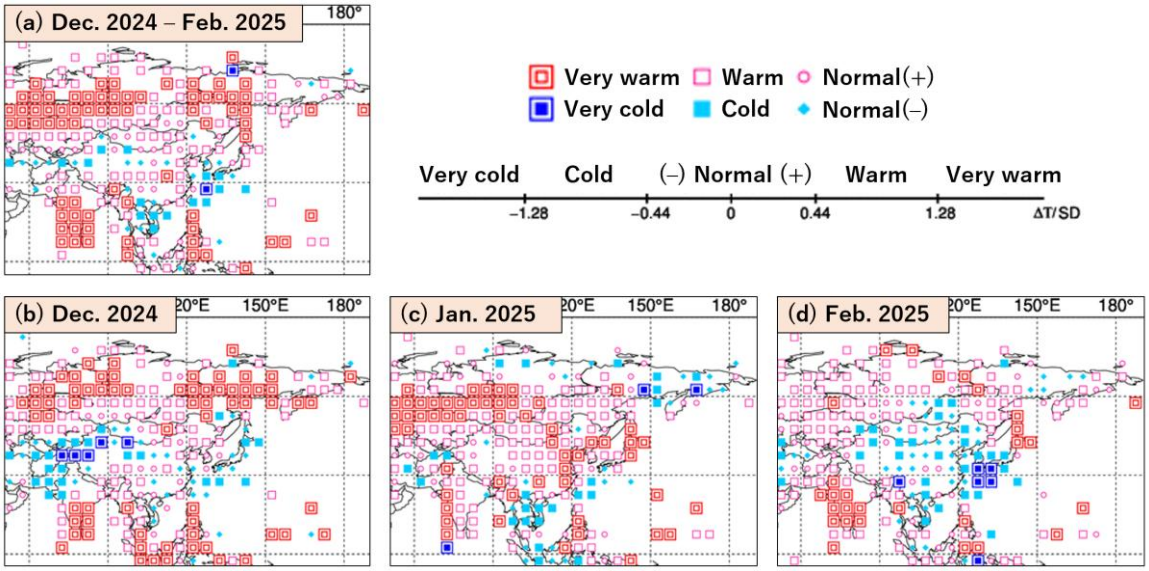

Figure 2-1 Temperature anomalies for (a) December 2024 to February 2025, (b) December 2024, (c) January 2025 and (d) February 2025

Categories are defined by the three-month/monthly mean temperature anomaly against the normal divided by its standard deviation and averaged in 5° × 5° grid boxes. The thresholds of each category are –1.28, –0.44, 0, +0.44 and +1.28. Standard deviations were calculated from 1991 – 2020 statistics. Areas over land without graphical marks are those where observation data are insufficient or where normal data are unavailable.

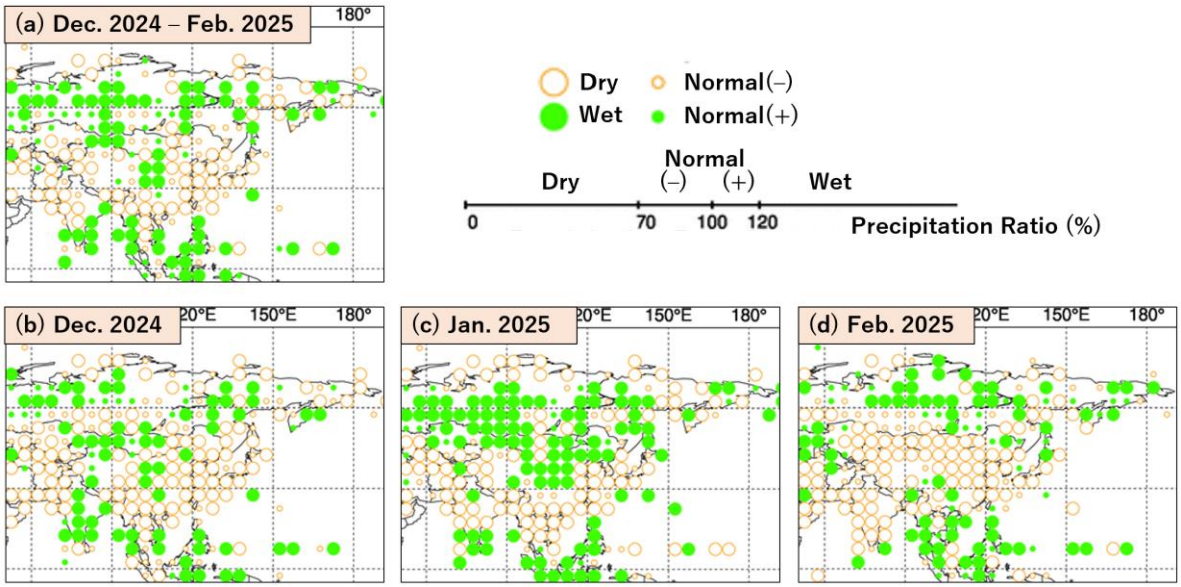

Figure 2-2 Precipitation ratio for (a) December 2024 to February 2025, (b) December 2024, (c) January 2025 and (d) February 2025

Categories are defined by the three-month/monthly precipitation ratio against the normal and averaged in 5° × 5° grid boxes. The thresholds of each category are 70, 100 and 120%. Areas over land without graphical marks are those where observation data are insufficient or where normal data are unavailable.

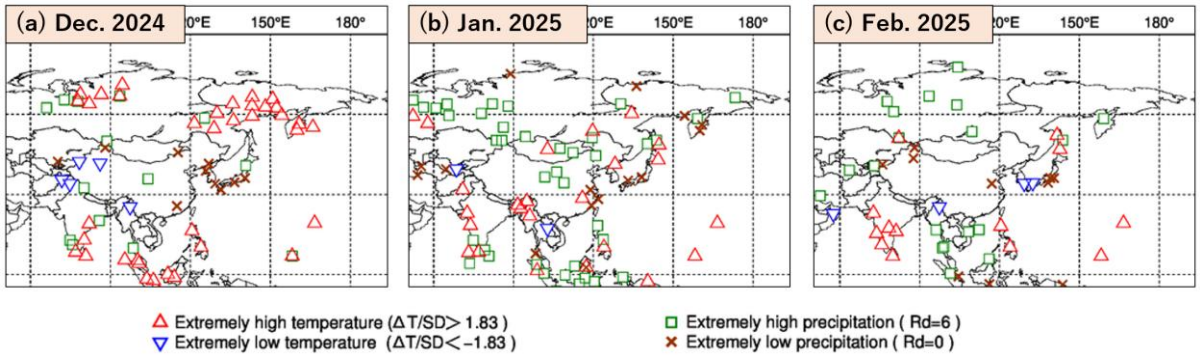

Figure 2-3 Extreme climate stations for (a) December 2024, (b) January 2025 and (c) February 2025

ΔT, SD and Rd indicate temperature anomaly, standard deviation and quintile, respectively.

Figure 2-3 plots stations where extreme climatic conditions were observed from December 2024 to February 2025. Extremely high temperatures were observed over parts of Siberia in December (Figure 2-3 (a)), and extremely high temperatures were observed over parts of South Asia and the Maritime Continent from December to February (Figure 2-3). Extremely low temperatures were observed over parts of East Asia particularly in December and February (Figures 2-3 (a) and (c)). Extremely high precipitation amounts were observed over wide areas of Siberia in January and February (Figures 2-3 (b) and (c)), and extremely low precipitation amounts were observed over parts of East Asia from December to February (Figure 2-3).

2. Characteristic atmospheric circulation and oceanographic conditions

This section presents characteristics of atmospheric circulation and oceanographic conditions averaged in winter 2024/2025.

2.1 Conditions in the tropics

Figure 2-4 shows three-month mean anomalies of sea surface temperature (SST), convective activity and upper-tropospheric large-scale divergence for winter 2024/2025. In the equatorial Pacific, positive SST anomalies were observed in western and eastern parts and negative SST anomalies were observed in central parts (Figure 2-4 (a)), resembling a La Niña Modoki-like pattern (Ashok et al. 2007). In the Indian Ocean, positive SST anomalies were observed in the Bay of Bengal, and negative SST anomalies were observed in western parts of the Arabian Sea. Convective activity inferred from OLR was enhanced from the eastern Indian Ocean to the Maritime Continent and in and around southern Central America, and suppressed from Africa to the central Indian Ocean and from the western to central equatorial Pacific (Figure 2-4 (b)), corresponding to the aforementioned SST anomalies. In the upper troposphere, large-scale divergence anomalies were dominant in and around the Maritime Continent and southern Central America, and large-scale convergence anomalies were seen from Africa to the central Indian Ocean and from the western to central tropical Pacific (Figure 2-4 (b)). Large-scale anomalous divergence promoted northward divergent wind anomalies from the Maritime Continent toward East Asia, partly contributing to northward deflection of the subtropical jet stream (STJ) over Eurasia as described later.

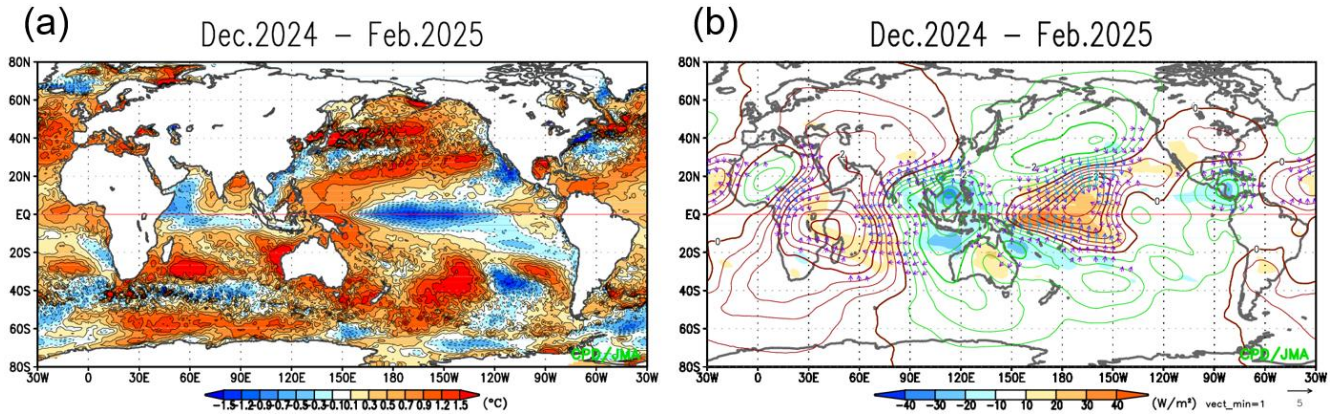

Figure 2-4 Three-month mean (a) SST anomalies and (b) anomalous convective activity in winter 2024/2025
The shadings in (a) and (b) show the SST anomalies [°C] and OLR anomalies [W/m^2]. The contours and vectors in (b) indicate 200-hPa velocity potential anomalies at intervals of 0.5 × 10^6 m^2/s and divergent wind anomalies, respectively. Negative (cold color) and positive (warm color) OLR anomalies show enhanced and suppressed convective activity compared to the normal, respectively.

Figure 2-5 shows three-month mean 200 and 850-hPa stream function anomalies in winter 2024/2025. In the upper troposphere, anti-cyclonic circulation anomalies straddling the equator were seen from the eastern Indian Ocean to the Maritime Continent (Figure 2-5 (a)), corresponding to a Matsuno-Gill response (Matsuno 1966, Gill 1980) to enhanced convection over the area. The northward deflection of the STJ accompanied by anti-cyclonic circulation anomalies in and around southwestern China was partly caused by the aforementioned northward divergent wind anomalies from the south (Figure 2-4 (b)). These tropical influences are supported by a Rossby wave source diagnosis (Sardeshmukh and Hoskins 1988) and the results of a numerical experiment conducted using a linear baroclinic model (Watanabe and Kimoto 2000, 2001; not shown). A wavy pattern of circulation anomalies was seen from southwestern China to Japan (Figure 2-5 (a)), indicating downstream propagation of Rossby wave packets along the STJ over Eurasia. The associated cyclonic circulation anomalies over Japan correspond to southward meandering of the STJ, partly contributing to a stronger-than-normal East Asian winter monsoon. In the lower troposphere, cyclonic circulation anomalies straddling the equator were seen over the Indian Ocean, and anti-cyclonic circulation anomalies straddling the equator were seen from the western to central Pacific (Figure 2-5 (b)), corresponding to a

Matsuno-Gill response to anomalous convection from the eastern Indian Ocean to the central equatorial Pacific.

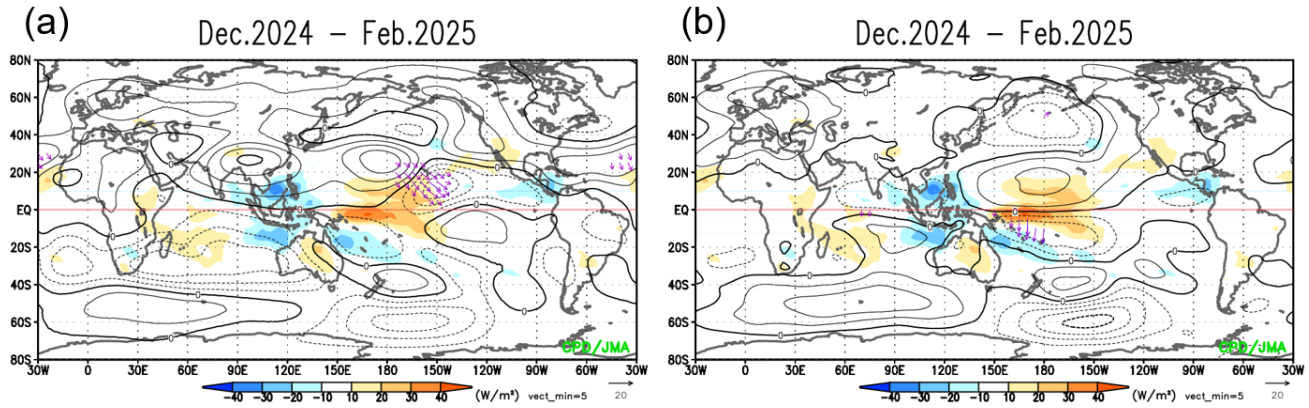

Figure 2-5 Three-month mean (a) 200-hPa and (b) 850-hPa stream function anomalies in winter 2024/2025

The contours indicate stream function anomalies at intervals of (a) 5×10^6 m^2/s and (b) 2.5×10^6 m^2/s, and the shadings show OLR anomalies [W/m^2]. The vectors denote horizontal component of wave activity flux [m^2/s^2] defined by Takaya and Nakamura (2001).

2.2 Conditions in the Northern Hemisphere extratropics

Figure 2-6 shows three-month mean 500-hPa height, sea level pressure (SLP), and 850-hPa temperature in winter 2024/2025 in the Northern Hemisphere. In the 500-hPa height field (Figure 2-6 (a)), positive anomalies were seen over Siberia, and negative anomalies were seen from Japan to the mid-latitude central North Pacific, corresponding to southward meandering of the polar front jet stream (PFJ) in and around Japan and a stronger-than-normal westerly jet over the North Pacific. In the SLP field, the Siberian High and the Aleutian Low were both stronger than normal, indicating a stronger-than-normal East Asian winter monsoon (Figure 2-6 (b)). Temperatures at 850 hPa were above normal over Siberia and below normal over southeastern East Asia (Figure 2-6 (c)), consistent with the 500-hPa height and SLP anomalies described above.

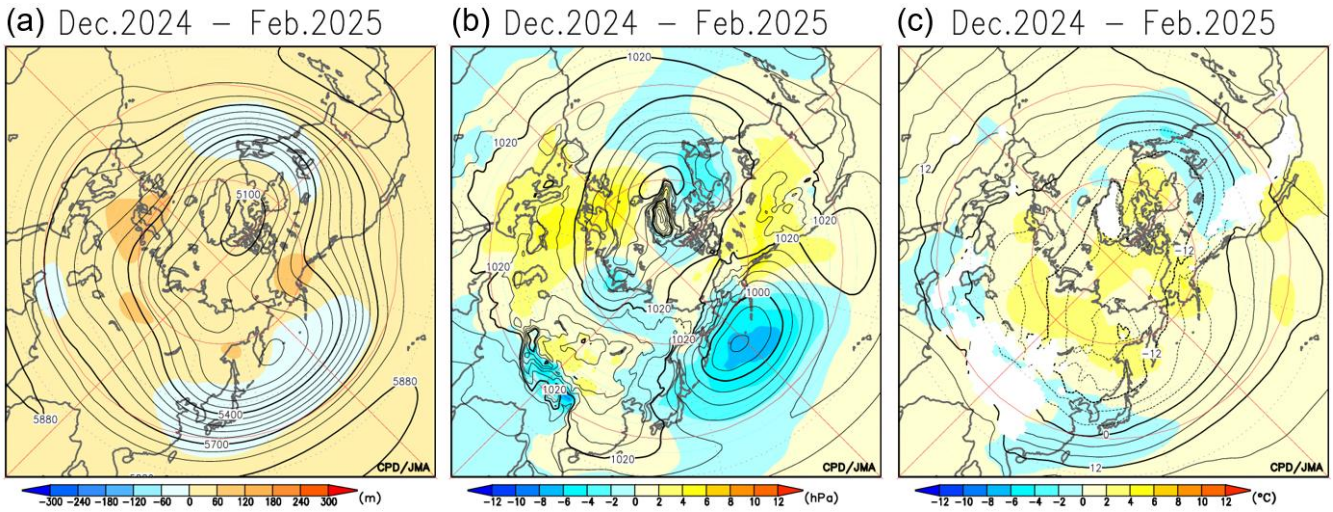

Figure 2-6 Three-month mean (a) 500-hPa height, (b) sea level pressure, and (c) 850-hPa temperature in winter 2024/2025

The contour intervals are (a) 60 m, (b) 4 hPa, and (c) 4 °C. The shading denotes related anomalies.

2.3 Cold spells in East Asia

As another notable winter characteristic, large sub-monthly temperature variations were seen in February 2025, accompanied by two cold spells in early February and the second half of the month. Although the stratospheric polar vortex was stronger than normal during winter (not shown), the polar vortex periodically split into two parts with a period of approximately two weeks in February (Figure 2-7 (a)). The influences of the split stratospheric polar vortex toward Greenland extended into tropospheric circulation anomalies from Greenland to Europe (Figures 2-7 (b) and (c)) through the processes of vertical coupling (e.g., Ambaum and Hoskins 2002, Perlwitz and Harnik 2004, Mukougawa and Hirooka 2007) and downward Rossby wave packet propagation (e.g., Kodera et al. 2008, Kodera et al. 2013). Circulation anomalies triggered by stratospheric variability propagated downstream along the PFJ and the STJ over Eurasia, causing southward meandering of the westerly jet around East Asia with negative height anomalies (Figures 2-8 (a) and (d)). Rossby wave propagation along the STJ was partly forced by enhanced convection over the region from the Indian Ocean to the Philippines. Concomitantly, both the Siberian High and the Aleutian Low were remarkably enhanced (Figures 2-8 (b) and (e)), promoting the outflow of cold air from Siberia to East Asia in early February and the second half of the month (Figures 2-8 (c) and (f)). In the period of two cold spells, a deepened trough with negative height anomalies at 500-hPa around East Asia contributed to amplification of the Aleutian High in the stratosphere via enhanced upward propagation of Rossby wave packets, recursively causing the above-mentioned periodic split of the stratospheric polar vortex. This stratosphere-troposphere interaction was potentially a primary factor behind the periodic cold spells observed in East Asia in February 2025.

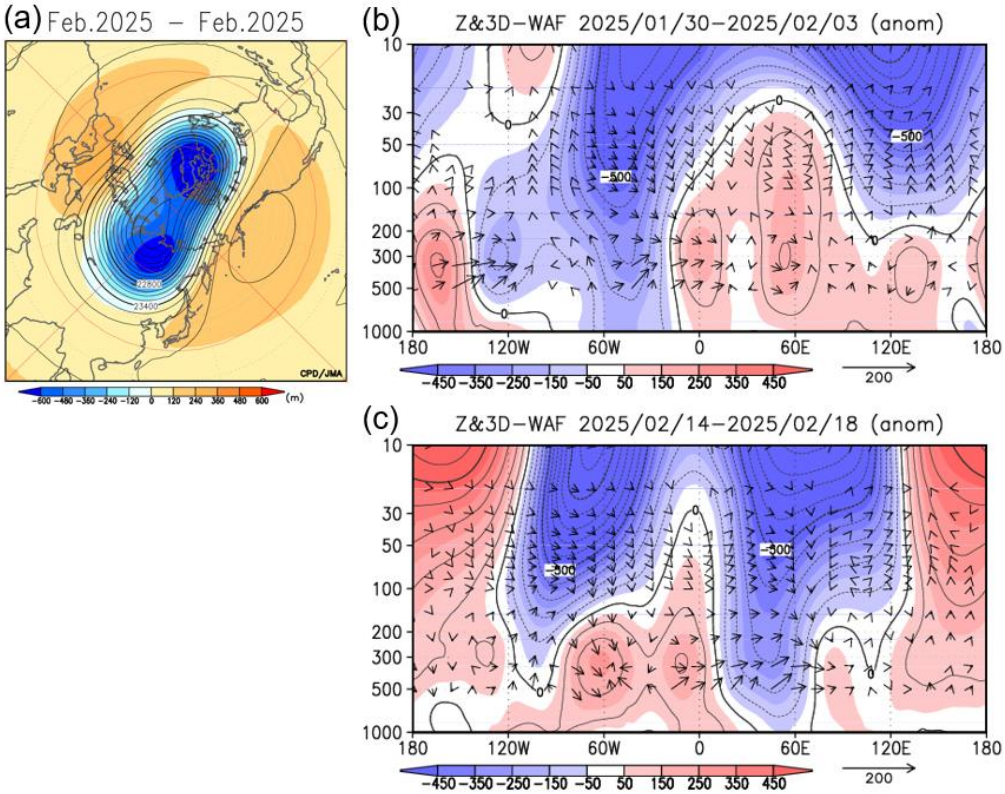

Figure 2-7 (a) 30-hPa height in February 2025. (b, c) Longitude-pressure cross section of height anomalies along 60°N averaged (b) from 30th January to 3rd February 2025 and (c) from 14th to 18th February 2025.

The contour intervals are (a) 120 m, (b, c) 100 m. The shading in (a) denotes related anomalies. The vectors in (b) and (c) indicate zonal and vertical components of wave activity flux defined by Takaya and Nakamura (2001).

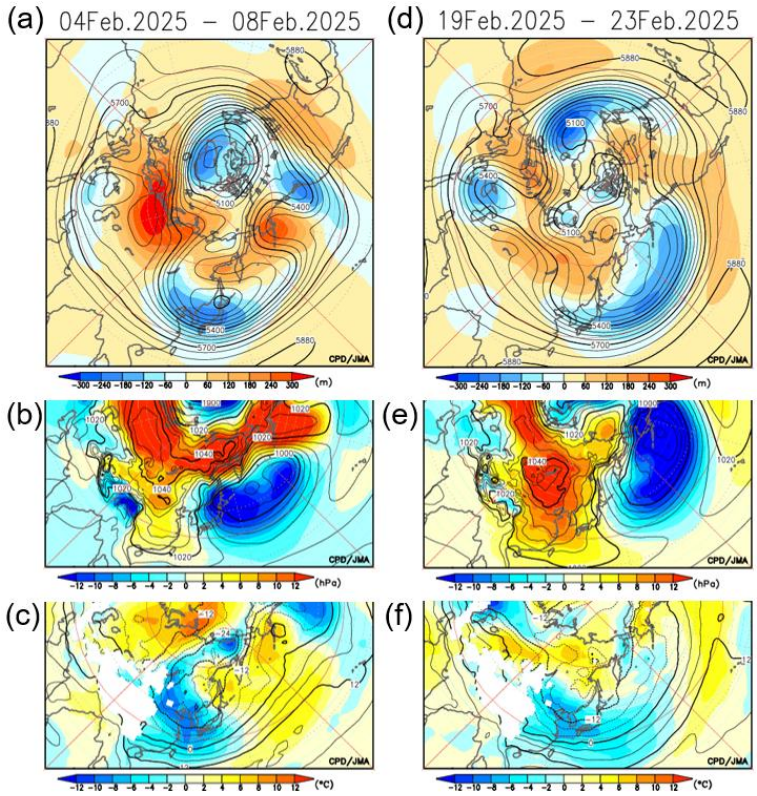

Figure 2-8 (a, d) 500-hPa height and (b, e) sea level pressure, and (c, f) 850-hPa temperature averaged (a, b, c) from 4th to 8th February 2025 and (d, e, f) from 19th to 23th February 2025.

The contour intervals are (a, d) 60 m, (b, e) 4 hPa, and (c, f) 4 °C. The shading denotes related anomalies.

References

Ambaum, M. H., and B. J. Hoskins, 2002: The NAO troposphere–stratosphere connection. *J. Climate*, **15**, 1969–1978, doi:10.1175/1520-0442(2002)015<1969:TNTSC>2.0.CO;2.

Ashok, K., S. K. Behera, S. A. Rao, H. Weng, and T. Yamagata, 2007: El Niño Modoki and its possible teleconnection. *J. Geophys. Res.*, **112**, C11007, https://doi.org/10.1029/2006JC003798.

Gill, A. E., 1980: Some simple solutions for heat-induced tropical circulation. *Quart. J. Roy. Meteor. Soc.*, **106**, 447–462.

Kurihara, Y., T. Sakurai, and T. Kuragano, 2006: Global daily sea surface temperature analysis using data from satellite microwave radiometer, satellite infrared radiometer and in-situ observations. *Weather Service Bulletin*, **73**, Special issue, s1–s18 (in Japanese).

Kodera, K., H. Mukougawa, and S. Itoh, 2008: Tropospheric impact of reflected planetary waves from the stratosphere. *Geophys. Res. Lett.*, **35**, L16806, doi:10.1029/2008GL034575.

Kodera, K., H. Mukougawa, and A. Fujii, 2013: Influence of the vertical and zonal propagation of stratospheric planetary waves on tropospheric blockings. *J. Geophys. Res. Atmos.*, **118**, doi:10.1002/jgrd.50650.

Kosaka, Y., S. Kobayashi, Y. Harada, C. Kobayashi, H. Naoe, K. Yoshimoto, M. Harada, N. Goto, J. Chiba, K. Miyaoka, R. Sekiguchi, M. Deushi, H. Kamahori, T. Nakaegawa; T. Y. Tanaka, T. Tokuhiro, Y. Sato, Y. Matsushita, and K. Onogi, 2024: The JRA-3Q reanalysis. *J. Meteor. Soc. Japan*, **102**, 49–109, https://doi.org/10.2151/jmsj.2024-004.

Matsuno, T., 1966: Quasi-geostrophic motions in the equatorial area. *J. Meteor. Soc. Japan*, **44**, 25–42.

Mukougawa, H., and T. Hirooka, 2007: Predictability of the downward migration of the Northern Annular Mode: A case study for January 2003. *J. Meteor. Soc. Japan*, **85**, 861–870.

Perlwitz, J., and N. Harnik, 2004: Downward coupling between the stratosphere and troposphere: The relative roles of wave and zonal mean processes. *J. Climate*, **17**, 4902–4909, doi:10.1175/JCLI-3247.1.

Sardeshmukh, P. D., and B. J. Hoskins, 1988: The generation of global rotational flow by steady idealized tropical divergence. *J. Atmos. Sci.*, **45**, 1228–1251, https://doi.org/10.1175/1520-0469(1988)045<1228:TGOGRF>2.0.CO;2.

Takaya, K., and H. Nakamura, 2001: A formulation of a phase-independent wave-activity flux for stationary and migratory quasigeostrophic eddies on a zonally varying basic flow. *J. Atoms. Sci.*, **58**, 608–627.

Watanabe, M., and M. Kimoto, 2000: Atmospheric-ocean thermal coupling in the North Atlantic: A positive feedback. *Quart. J. Roy. Meteor. Soc.*, **126**, 3343–3369.

Watanabe, M., and M. Kimoto, 2001: Corrigendum. *Quart. J. Roy. Meteor. Soc.*, **127**, 733–734.

(TAKEMURA Kazuto, YAMADA Ken, Tokyo Climate Center)

<<Table of contents <Top of this article

TCC and WMC Tokyo co-contributions to Regional Climate Outlook Forums in Asia

WMO Regional Climate Outlook Forums (RCOFs) bring together national, regional and international climate experts on an operational basis to produce regional climate outlooks based on inputs from participating NMHSs, regional institutions, Regional Climate Centres (RCCs) and global producers of climate predictions. By providing a platform for countries with similar climatological characteristics to discuss related matters, these forums ensure consistency in terms of access to and interpretation of climate information. In spring 2025, TCC experts participated in the following two RCOFs in Asia.

- The 31st summer session of the South Asian Climate Outlook Forum (SASCOF-31)
- The 21st session of the Forum on Regional Climate Monitoring, Assessment and Prediction for Regional Association II (FOCRA II)

1. SASCOF-31

RCC Pune hosted the 31st summer session of the South Asian Climate Outlook Forum (SASCOF-31) and Climate Services User Forum (CSUF) from 28 to 30 April 2025 in Pune, India. As part of WMO World Meteorological Centre (WMC) and TCC joint activities (co-activities), a JMA expert made two presentations as detailed below. These contributed to discussions on the climate outlook for South Asia, and are expected to support the output of country-scale outlooks by National Meteorological and Hydrological Services (NMHSs) in the relevant regions.

- Summer monsoon season outlook based on JMA's operational seasonal ensemble prediction system (JMA/MRI-CPS3) with probabilistic information on oceanographic conditions from the Indian Ocean to the Pacific (El Niño southern oscillation, Indian Ocean Dipole, etc.) and associated atmospheric circulation patterns

- Recent joint activities involving WMC Tokyo and TCC roles, such as the launch of TCC's Three-month Guidance Tool (TCC News No. 77) and capacity development in East Asia

SASCOF-31 issued a climate outlook for the 2025 summer monsoon season (June – September). The subsequent CSUF session focused on interfacing with users from the water, agriculture, disaster risk reduction and health sectors for interpretation and assessment of seasonal climate information and elucidation of specific needs toward the provision of further customized climate information.

At the SASCOF meeting

At the CSUF meeting

Commendation for chairing the session
(provided by SASCOF)

Group photo at the conference center (provided by SASCOF)

2. FOCRA II

The 21st Session of the Forum on Regional Climate Monitoring, Assessment and Prediction for Asia (FOCRA II) was held from 14 to 16 May 2025 in Qingdao, Shandong, China. This meeting was attended by 135 representatives from the WMO Secretariat and over 20 countries and regions, including Asia, the United Kingdom, the Pacific Islands, the Caribbean and Africa. Attendees shared recent research results and discussed climate service development, new technologies and applications such as AI, and climate projection and seasonal climate prediction.

JMA representatives gave three presentations on the following and led discussions in a chairing role:

- Recent WMC Tokyo/TCC activities, including the pilot launch of seasonal tropical cyclone forecast products,

publication of Climate Change in Japan 2025, and implementation of an annual training seminar

- Climate monitoring diagnosis results for winter 2024/25 based on discussions by JMA's Advisory Panel on Extreme Climate Events
- Seasonal outlook for summer over Japan, including probabilistic forecasts, based on oceanographic conditions from the Indian Ocean to the Pacific and associated atmospheric circulation patterns predicted by JMA/MRI-CPS3

FOCRA II issued a consensus outlook for summer climate conditions in the RA II region after discussions in the summary session. Broad agreement was reached on enhancing collaboration between RCCs and NMHSs toward the production of enhanced climate information for RA II.

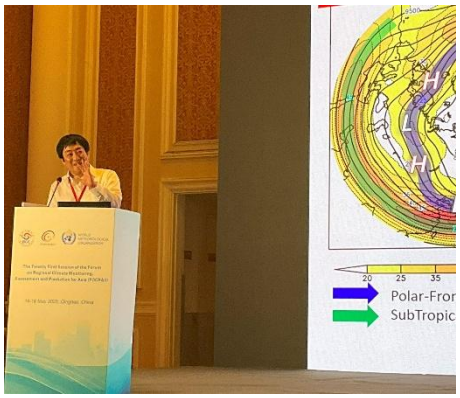

Presentation at FOCRA II

Discussions at FOCRA II

Discussions at FOCRA II

Group photo (provided by FOCRA II)

(SASCOF-31: YAMADA Ken, FOCRA II: MAEDA Shuhei and UMEZU Hironori, Tokyo Climate Center)

<<Table of contents <Top of this article

You can find the latest newsletter from the Japan International Cooperation Agency (JICA).

JICA Magazine

https://jicamagazine.jica.go.jp/en/

"JICA magazine" is a public relations magazine published by JICA. It introduces the current situations of developing countries around the world, the people who are active in the field, and the content of their activities.

Any comments or inquiry on this newsletter and/or the TCC website would be much appreciated.
Please e-mail to tcc@met.kishou.go.jp.
(Editors: HARADA Masashi, KURAMOCHI Masaya)

Tokyo Climate Center, Japan Meteorological Agency
3-6-9 Toranomon, Minato City, Tokyo 105-8431, Japan

TCC Website:
https://www.data.jma.go.jp/tcc/tcc/index.html